Nonequilibrium Polymer Rheology in Spin-Cast Films

David R. Barbero and Ullrich Steiner*

Department of Physics, Nanoscience Centre, University of Cambridge, J J Thomson Avenue, Cambridge CB3 0HE, United Kingdom

(Received 18 December 2008; published 18 June 2009)

A new experimental approach is introduced to probe the rheology of ≳100 nm-thick liquid polymer films. As-cast films were found to have a substantially reduced effective viscosity compared to annealed films. The reduced viscosity is explained in terms of nonequilibrium chain conformations giving rise to a reduced entanglement density caused by the rapid quenching of the film during spin coating. Unexpectedly long annealing times at high temperatures are required for the films to recover their bulk rheology.

DOI: 10.1103/PhysRevLett.102.248303 PACS numbers: 83.80.Rs, 68.15.+e, 68.60.−p, 83.50.−v

Spin-cast films are ubiquitous in polymer science and technology. While relatively thick films (≳100 nm) are usually described in terms of the polymer bulk properties, thinner films often break up at temperatures much below their bulk glass transition temperature T_g [1–5]. Some studies have reported a surprisingly abnormal rheological behavior also for ~100 nm thick films [3–5], while elastic stresses were shown to drive the formation of holes in thin supported films [6–9]. The control of the rheological properties is essential for many thin film technologies.

The present study addresses a system that is commonly thought to possess a bulklike rheology: ≳100 nm-thick spin-cast polystyrene (PS) films above the glass transition temperature of PS (~105 °C). We use electric fields to weakly perturb the free surface of the polymer melt [10]. By measuring the characteristic time for the formation of a surface wave, we are able to directly probe the effective viscosity of liquid polymer films. This experiment controls the destabilization of films that otherwise stay intact upon heating above T_g, thereby enabling the direct comparison of as-cast with equilibrated films. This is in contrast to the commonly used dewetting experiments which require intrinsically unstable films that cannot be equilibrated prior to the measurement.

The experimental setup consisted of two parallel plates which function as plate capacitor and optical cavity (Fig. 1), a polished silicon wafer and an indium tin oxide (ITO) covered glass slide. 90–148 nm thick PS films (Table I) were spin cast from filtered toluene solutions onto cleaned wafers. An electrically insulating layer (SU8) was deposited onto the cleaned ITO slide, which was then placed onto the silicon substrate with the ITO facing the polymer film. A small air gap of ~0.2–1 μm was created between the plates by the sparse deposition of silicon oxide colloids onto the film before assembly. The device was placed in a homemade oven which was mounted onto an inverted optical microscope with monochromatic illumination (515 nm) for *in situ* observation of the film. A slight misalignment of the two plates resulted in a slight wedge geometry (≤0.01°), giving rise to parallel interference fringes in reflection [12]. The plate spacing d was measured *in situ* by interferometry and after the experiments by atomic force microscopy.

The assembly was heated to $T > T_g$ and a voltage was applied to the two plates, defining the start of the experiment ($t = 0$). The experimental parameters are given in Table I and as insets in Fig. 2. The interference pattern was monitored using a CCD camera. The onset of a surface wave on the polymer film gave rise to a distortion of the linear interference pattern, which was used to reconstruct the real-space surface pattern. Local thickness changes as small as 1 nm can be resolved by measuring the phase shift in the interference pattern. This yields the time dependence of the emerging surface undulation $h(x, t)$ triggered by the applied electric field [13].

The pressure arising from an electric field applied perpendicular to a liquid-air surface consists of the destabilizing electrostatic pressure p_{el} which is opposed by the restoring Laplace pressure p_{Lap} [14]

$$p(h) = p_{\mathrm{el}} + p_{\mathrm{Lap}} = -\frac{\varepsilon_0 \varepsilon_p (\varepsilon_p - 1) U^2}{[\varepsilon_p (d - h) + h]^2} - \frac{\gamma \partial^2 h}{\partial x^2}, \quad (1)$$

with γ and ε_p the surface tension and dielectric constant of the polymer, respectively ($\varepsilon_{\mathrm{PS}} = 2.5$, $\gamma_{\mathrm{PS}} = 27.5$–$32.7$ mN/m), and ε_0 the vacuum permittivity. This pressure couples to thermal thickness fluctuations in the film. In the limit where the surface amplitude is much smaller than the wavelength of the instability λ and the

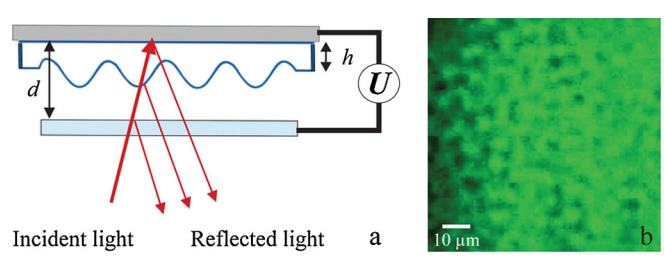

FIG. 1 (color online). (a) Schematic of the experimental setup. The polymer film is sandwiched between two parallel plates, which serve simultaneously as plate capacitor electrodes and as an optical cavity. (b) Image of the onset of an electric field driven surface instability with $\lambda \sim 7$ μm.

 © 2009 The American Physical Society

TABLE I. Experimental parameters of the data in Fig. 2.

	M_w (kg/mol)	Figure 2	η (kPa s)[a]	T_{ann} (°C)	t_{ann} (h)
$PS_{27.5}$	27.5	a	2.2[b]	···	···
$PS_{27.5}$	27.5	b	10.6[c]	145	~22
PS_{113}	113	c	5.5[b]	···	···
PS_{113}	113	d	32.3[d]	155	145
PS_{655}	655	e	0.2[b,e]	···	···
PS_{10}	10	f	13[c]	120 □	40 □

[a]At the temperature given in Fig. 2.
[b]Fit to data of Fig. 2.
[c]Measured using a plate rheometer.
[d]From [11].
[e]Bulk viscosity: 1.3 MPa s calculated from [11].

film thickness h, the perturbation of the film is governed by a linear stability analysis [14,15], resulting in the development of a dominant mode with

$$\frac{\lambda}{\lambda_0} = 2\pi\left(\frac{E_p}{E_0}\right)^{-3/2}, \tag{2}$$

where $E_p = U(\varepsilon_p d - (\varepsilon_p - 1)h_0)^{-1}$ is the electric field in the polymer layer. $E_0 = U/\lambda_0$ and $\lambda_0 = \varepsilon_0\varepsilon_p(\varepsilon_p - 1)^2 U^2 \gamma^{-1}$ are the characteristic values of E_p and λ. λ accurately reflects the balance of forces acting on the free interface, irrespective of the film rheology [14]. The characteristic time for the onset of the instability

$$\tau = \tau_0 \pi^4 \left(\frac{E_p}{E_0}\right)^{-6} = \frac{3}{(2\pi)^4}\frac{\eta}{\gamma}\frac{\lambda^4}{h_0^3}, \tag{3}$$

on the other hand, is proportional to the viscosity η. The observation of the evolution of an electrohydrodynamic surface wave therefore allows us to disentangle the force balance driving the instability from the rheology within the film, providing an effective way to probe the flow in thin liquid layers.

The sample was observed until a small surface undulation with wavelength λ and height (peak to valley) of ~5 nm appeared after a time t. For these parameters, the conditions for the linear stability analysis hold and Eq. (3) can be used to calculate τ. Because of the wedge geometry of the two plates, a constant applied voltage U caused a weak lateral variation of the electric field. Several values of τ and λ can thus be measured at different lateral positions on the sample as the instability develops.

Representative data sets are shown in Fig. 2 for films of the four polymers used in this study. Figures 2(a) and 2(c) correspond to as-cast films of $PS_{27.5}$ and PS_{113}. The dashed lines are the predictions of Eq. (3) using tabulated values for the surface tension and dielectric constant of PS and measured viscosities. The two data sets fall significantly below the prediction of Eq. (3), with a deviation that increases with molecular weight. The reduced value in τ reveals an unexpectedly high mobility of the film.

The derivation of Eq. (3) assumes a zero flow velocity of the polymer at the substrate. The inclusion of finite slip at the liquid-solid interface into Eq. (3) is predicted to lead to

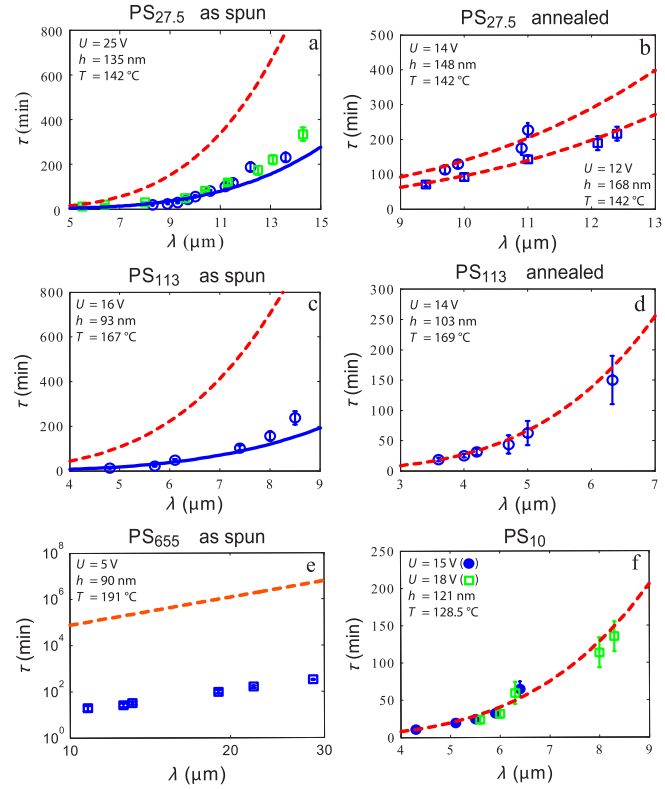

FIG. 2 (color online). Characteristic destabilization time τ vs λ. (a),(c) and (b),(d) compare films before and after annealing for $PS_{27.5}$ and PS_{113}. The different symbols correspond to bare and SAM covered substrates in (a), samples of different thicknesses in (b), annealed and as-cast samples in (f). The dashed lines are predictions of Eq. (3) using the bulk viscosity, the solid lines are fits of Eq. (3) by variation of η (Table I).

a reduction in τ. We tested the role of the substrate by using silicon wafers that were functionalized with a hexamethyldisilazane self-assembled monolayer, which reduced the interfacial energy of the silicon substrate. Although the functionalized substrate had a substantially lowered interfacial energy with PS compared to the bare silicon wafer, the characteristic destabilization times are indistinguishable [Fig. 2(a)]. This indicates that the solid boundary does not play a significant role during the early stage of destabilization. A small undulation at the free surface does not give rise to sufficiently high stresses at the substrate to cause interfacial slip.

From Eq. (3), the only likely parameter that is able to account for the increased film mobility is therefore the effective viscosity η. For the as-cast films, the solid lines in Fig. 2 are fits of Eq. (3) to the data, postulating a viscosity reduction by factors of 5 and 6 for $PS_{27.5}$ and PS_{113}, respectively. Experiments with a much higher molecular weight polymer in Fig. 2(e) show an effective viscosity reduction by nearly 4 orders of magnitude. Since the measured bulk viscosities agree with the literature values for PS, the only likely explanation for the mobility reduction in Fig. 2 arises from nonequilibrium effects caused by the film deposition procedure. To test this

hypothesis, films cast from $PS_{27.5}$ and PS_{113} were heated at $T > T_g$ for times between 22 and 145 h (Table I). The comparison of destabilization experiments in Fig. 2(b) with the prediction of Eq. (3) confirms that bulk viscosity in the films is recovered after annealing. The good agreement of experiments and prediction validates our experimental approach. It also indicates that high molecular weight polymer chains in spin-cast films have a quenched structure that gives rise to a significantly lowered effective viscosity. The long time annealing of the film removes this nonequilibrium effect. The destabilization of PS_{10} films which have a M_w below the entanglement molecular weight M_e of PS in Fig. 2(f) does not show this effect: the data for as-cast and annealed films are both described by the bulk viscosity.

The sketch in Fig. 3 illustrates a possible mechanism that is able to account for the nonequilibrium behavior in spin-cast films. In the initial phase of spin coating the polymer forms a semidilute solution in a good solvent. During spinning, the solvent rapidly evaporates, increasing the polymer concentration in the film. In thermal equilibrium, the number of entanglements per chain with surrounding chains increases with polymer concentration. This leads to an increasingly entangled semidilute solution with decreasing solvent concentration. Since this increase in entanglements can only occur by chain reptation, the mobility of the chains must be high enough for the entanglement density to increase further. With increasing polymer concentration this process is progressively slowed down and comes to a stop when the glass transition of the coils is reached. At this point, the film still contains $(10\text{–}20)\%_{\mathrm{vol}}$ solvent, which mostly evaporates during the late stage of spin coating [16]. The slowdown of chain mobility and chain collapse is therefore likely to give rise to an entanglement density per chain which is lower compared to the melt equilibrium. Since the melt viscosity of polymers arises from the entangled nature of the chains, this qualitatively explains the lowered effective viscosity of the as-cast films. Annealing the film at $T > T_g$ for times exceeding the reptation time equilibrates the chains to their fully entangled nature of the equilibrated melt.

The results in Fig. 2 indicate that the times required to destabilize the films were below the relaxation times of the chains. Careful examination of the data in Figs. 2(a) and 2(c) shows that the data for large values of λ (low applied electric fields) lie above the curve fitted to the data with small λ. This is probably due to chain relaxation during the experiment. This effect is better seen when plotting the two PS_{113} data sets in terms of the stress-strain relation in Fig. 4(a) for the onset of the instability. The lateral stress arises from the difference in pressure [Eq. (1)]: $\sigma = 2[p(h_{\max}) - p(h_{\min})]$, where $h_{\max}$, $h_{\min}$ correspond to lateral locations x of adjacent undulation maxima and minima. This pressure difference gives rise to a relative thickness change of $2\Delta h = h_{\max} - h_{\min}$ over a lateral distance $\lambda/2$ during the time interval τ, defining the strain rate.

The linear stress-strain relation extracted from the data in Fig. 2(d) for the annealed PS_{113} films is characteristic for a Newtonian liquid [15] with a viscosity of $\eta = 29$ kPa s, in good agreement with the literature value (Table I). The data of Fig. 2(c), for the as-cast film, on the other hand, shows a nonlinear stress-strain variation with a much smaller slope. In this representation, high strain rates correspond to small values of τ, while long destabilization times give rise to low strain rates. The lowest value of the slope at high strain rates corresponds to the much lowered effective viscosity of the data in Fig. 2(c) for small values of τ (high destabilizing fields). The increase in slope (i.e., increase in viscosity) with decreasing strain rate (i.e., low fields and high values of τ) is indicative of an increase in relaxation of the quenched polymer chains, giving rise to increasing values of the effective viscosity. The two curves approach each other in the limit of very low strain rates.

The connection between the reduction in entanglement density of the chains in the as-cast films and their lowered viscosity can be quantified in terms of the reptation model [17], $\eta = \eta_0(M_w/M_e)^\nu$ with the intrinsic viscosity of the unentangled melt η_0. Comparing two polymer melts with the same chain length but different degrees of entanglement, M_e and M_e', can therefore be described by the relation $M_e'/M_e = (\eta'/\eta)^{-k}$, with $k = 1/(\nu - 1)$. Using the commonly accepted values of $\nu = 3.4$ and $M_e \approx 17$ kg/mol for PS, an increase in M_e' to ≈ 29 kg/mol and ≈ 36 kg/mol account for the effective viscosity decrease in the $PS_{27.5}$ and PS_{113} films, respectively.

The viscosity reduction in our experiments is likely to arise from a reduced entanglement density. However, an-

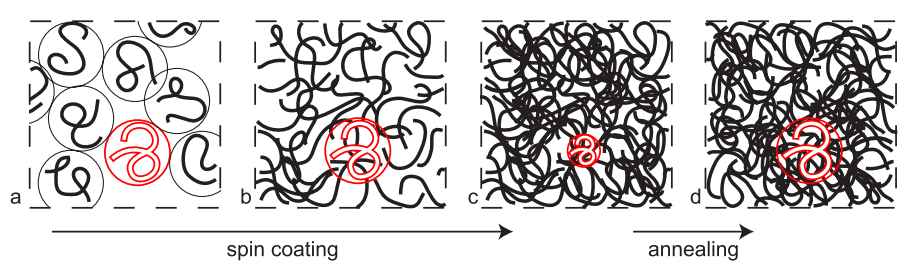

FIG. 3 (color online). Model for the reduction in effective viscosity in spin-cast films. (a) Starting from a semidilute solution, (b) the chains start to entangle as the concentration increases. (c) The slowdown and collapse of the chains for high polymer concentrations prevents the full equilibration of the chains. Thermal annealing equilibrates the chains, restoring the melt entanglement density (d).

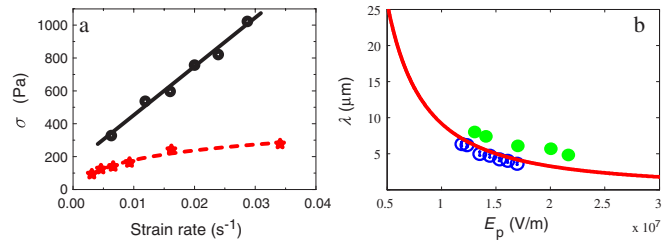

FIG. 4 (color online). (a) Lateral stress vs strain rate induced by the film destabilization in as-cast (★) and annealed (●) PS_{113} films. (b) Characteristic wavelength vs the electric field, E_p, for as-cast (●) and annealed (○) PS_{113} films.

nealing times significantly exceeding the reptation time were needed to recover bulk rheology in the thin films. In particular, the annealing of PS_{655} films for over one week did not recover the PS bulk viscosity. This indicates that the thermal equilibration of very high M_w films by thermal annealing cannot be achieved in technologically practical times. Despite the high film thickness, the quenched polymer chains seem to equilibrate substantially more slowly than predicted by the reptation model. Relaxation processes exceeding the reptation time have previously been observed in a number of systems [18–21], but remain unexplained.

The spin-cast chains may have quenched conformations that cannot be equilibrated by a standard reptation process. The Edwards reptation time is the characteristic time for tube renewal of a Gaussian coil in an equilibrated melt. The equilibration of quenched chains may, however, be kinetically hindered. In particular, chains that have internal entanglements (knots) may have relaxation times much above the Edwards reptation time [22]. While the detailed entanglement dynamic of chains during spin coating is unknown, our experiments indicate that frustrated coil structures are formed, which equilibrate much slower than predicted by reptation theory.

A further aspect of nonequilibrium chain formation is frozen-in in-plane stresses, found in much thicker films [16] and in dewetting experiments [9]. A recent theoretical study predicts that in-plane stresses in thin films can drive a film instability [23]. In our experiments the presence of in-plane stored tensile stresses in the as-cast films is therefore expected to act as an additional driving force. Compared to the annealed, stress-free films this should result in a film instability with smaller values of λ in the as-cast film. Figure 4(b) compares the experimentally determined instability wavelength of as-cast and annealed films as a function of the electric field E_p. While the data for the annealed films are well described by the prediction of the linear stability analysis (line), the values of λ are systematically *larger* in the as-cast film, indicating a stabilizing pressure. Possible explanations for this stabilizing pressure include a variation of the entanglement density normal to the film surface caused by solvent evaporation or by polymer adsorption at the substrate, overpowering destabilizing in-plane stresses that may form during spin coating.

In conclusion, we have used an electric field technique to weakly perturb the surface of ~100 nm thick PS films. As-cast films of sufficiently high molecular weight exhibit a faster than expected mobility. Long time annealing of the films reduces their mobility to the expected value. The mobility reduction is explained in terms of nonequilibrium conformations of the chains in the as-cast films, caused by the rapid solvent evaporation during spin coating, which results in a lowered entanglement density and in a reduced effective viscosity. The reentanglement of the chains by annealing was found to be substantially longer than the reptation time. The experiments also show an unexpected weak stabilization of the as-cast films. The substantial change in viscosity in polymer films compared to their bulk rheology is likely to significantly influence the processing of deposited films.

We thank G. Reiter and E. Raphael for stimulating discussions and the EU RTN-6 network "Patterns" for financial support.

*Also at Freiburg Intitute for Advanced Studies, University of Freiburg, Germany.
u.steiner@phy.cam.ac.uk

[1] G. Reiter, Phys. Rev. Lett. **68**, 75 (1992).
[2] J. L. Keddie *et al.*, Europhys. Lett. **27**, 59 (1994).
[3] J. H. Teichroeb and J. A. Forrest, Phys. Rev. Lett. **91**, 016104 (2003).
[4] T. Kerle *et al.*, Macromolecules **34**, 3484 (2001).
[5] Z. Fakhraai and J. A. Forrest, Science **319**, 600 (2008).
[6] T. Vilmin and E. Raphaël, Europhys. Lett. **73**, 906 (2006).
[7] S. Gabriele *et al.*, Phys. Rev. Lett. **96**, 156105 (2006).
[8] G. Reiter and P.-G. de Gennes, Eur. Phys. J. E **6**, 25 (2001).
[9] P. Damman *et al.*, Phys. Rev. Lett. **99**, 036101 (2007).
[10] E. Schäffer *et al.*, Nature (London) **403**, 874 (2000).
[11] T. G. Fox and P. J. Flory, J. Appl. Phys. **21**, 581 (1950).
[12] The lateral stress caused by the wedge geometry is less than 3% of the lowest stress in Fig. 4(a).
[13] D. R. Barbero and U. Steiner (to be published).
[14] E. Schäffer *et al.*, Europhys. Lett. **53**, 518 (2001).
[15] The treatment of the polymer melt as a Newtonian fluid in [14] is limited to very low flow rates.
[16] S. G. Croll, J. Appl. Polym. Sci. **23**, 847 (1979).
[17] M. Doi and S. F. Edwards, *The Theory of Polymer Dynamics* (Oxford University Press, Oxford, 1986).
[18] H. Bodiguel and C. Fretigny, Eur. Phys. J. E **19**, 185 (2006).
[19] T. Kanaya *et al.*, Polymer **44**, 3769 (2003).
[20] C. G. Robertson *et al.*, Macromolecules **37**, 10 018 (2004).
[21] W. Rong *et al.*, J. Polym. Sci. B **43**, 2243 (2005).
[22] S. R. Quake, Phys. Rev. Lett. **73**, 3317 (1994).
[23] T. Vilmin and E. Raphaël, Phys. Rev. Lett. **97**, 036105 (2006).